

Efficient spin-current injection in single-molecule magnet junctions

Haiqing Xie,¹ Fuming Xu,^{2,*} Hujun Jiao,³ Qiang Wang,^{1,†} and J.-Q. Liang³

¹Department of Physics, Taiyuan Normal University, Taiyuan 030001, China

²College of Physics and Energy, Shenzhen University, Shenzhen 518060, China

³Institute of Theoretical Physics, Shanxi University, Taiyuan 030006, China

(Dated: December 14, 2024)

We investigate spin-polarized transport through a single-molecule magnet (SMM) in the sequential and cotunneling regimes, where the SMM is weakly coupled to one ferromagnetic and one normal-metallic leads. It is found that the spin polarization injected from the ferromagnetic lead is amplified and highly polarized spin-current can be generated, due to the exchange coupling between the conduction electron and the anisotropic spin of the SMM. Moreover, the spin-current polarization can be tuned by the gate or bias voltage, and thus an efficient spin injection device based on the SMM is proposed in molecular spintronics.

PACS numbers: 75.50.Xx, 75.70.Tj, 73.23.-b, 72.25.-b, 85.75.d

I. INTRODUCTION

As is well known, the efficient generation and manipulation of spin-polarized current are the crucial elements in the field of spintronics.¹ Considerable efforts have been devoted to direct spin-current injection from ferromagnetic (FM) electrodes into nonmagnetic materials via tunnel junctions, such as graphene,^{2,3} silicon,⁴ and quantum dots (QDs).^{5–8} It is shown both experimentally^{5,6} and theoretically⁷ that the spin-current polarization can be electrically manipulated in transport through a single QD weakly coupled to one FM and one normal-metallic (NM) electrodes, but the polarization is limited by the typical polarization of ferromagnet with 30 – 40%.⁹ Interestingly, when the coupling of the FM lead with the QD is much stronger than that of the NM lead, the polarization of spin injection in the strong coupling regime is greatly enhanced, far beyond the intrinsic polarization of ferromagnets,⁸ due to the FM exchange-field induced spin-splitting of the QD level. However, high spin polarization strongly depends on the left-right asymmetry of the QD-lead coupling in this case.

In molecular spintronics, single-molecule magnets (SMMs) with a large molecular spin have magnetic bistability induced by the easy-axis magnetic anisotropy, which has potential application in data storage and information processing. Therefore, transport properties through SMMs have been intensively investigated in recent years.^{10–12} It is both theoretically^{13–18} and experimentally¹⁹ verified that, the spin switching of SMM can be realized by spin-polarized currents. Moreover, the tunnel magnetoresistance effect of SMM has been theoretically studied in sequential, cotunneling,^{20,21} and Kondo regimes.^{22,23} Very recently, Natterer *et al.* have achieved reading and writing operations of spin states of magnetic holmium atoms at the atomic level in experiment.²⁴ On the other hand, spin-polarized current itself can exhibit spin-diode,²⁵ negative differential conductance and,²⁶ memory behaviors.²⁷ Specifically, the spin-filter effect^{28,29} and thermoelectric induced pure spin-current^{30,31} are found in SMMs with nonmagnetic

leads.

In this paper, we adopt the master equation approach to study spin-current injection in a SMM coupled to one FM and one NM leads in the weak coupling regime. The system under investigation is shown in Fig. 1, the magnetization of FM lead is collinear with the magnetic easy axis of the SMM. Experimentally, this transport setup can be realized on a FM scanning tunneling microscope tip coupled to a magnetic adatom or SMM placed on a NM surface.^{11,15,19,25,32} The SMM is modeled as a single-level QD with a local uniaxial anisotropic spin.^{13,20} Both FM and antiferromagnetic (AFM) exchange couplings are discussed in this work. As in the case of FM-QD-NM system,⁷ the electron transport is rather asymmetric with respect to the reversal of bias voltage.^{25,32} For negative bias voltages $V < 0$, the electrons flow mainly from the FM lead into NM lead, while the situation is opposite for $V > 0$. Owing to the easy-axis magnetic anisotropy of SMM and spin-flip processes,^{20,21,32,33} we find that the spin-current polarization can be dramatically enhanced.

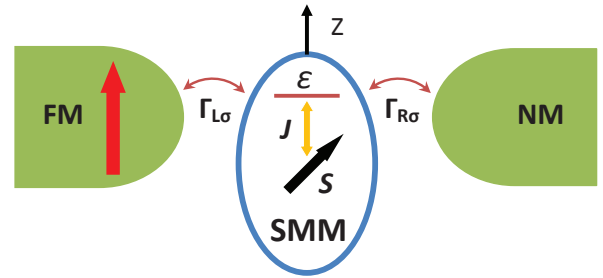


FIG. 1: (Color online) Schematic diagram for a SMM weakly coupled to FM and NM electrodes. The magnetization of FM lead is collinear with the easy axis of SMM (assumed as z -axis). Bias voltages $V/2$ and $-V/2$ are applied on the left (L) and right (R) electrodes, respectively.

II. MODEL AND METHOD

The total Hamiltonian of the SMM tunnel junction shown in Fig. 1 is written as

$$H = H_{SMM} + H_{leads} + H_T. \quad (1)$$

The first term is the giant-spin Hamiltonian of the SMM^{13,16,20}

$$H_{SMM} = \sum_{\sigma} (\varepsilon - eV_g) d_{\sigma}^{\dagger} d_{\sigma} + U d_{\uparrow}^{\dagger} d_{\uparrow} d_{\downarrow}^{\dagger} d_{\downarrow} - K(S^z)^2 - J\mathbf{s} \cdot \mathbf{S}. \quad (2)$$

Here, ε is the energy of the orbital level (OL) of the magnetic molecule, which can be tuned by the gate voltage V_g , and the operator d_{σ}^{\dagger} (d_{σ}) creates (annihilates) an electron with spin σ in the molecular OL. U is the Coulomb energy of the two electrons in the molecule, and K ($K > 0$) denotes the easy-axis anisotropy of the SMM. The spin operator of the OL is defined as $\mathbf{s} \equiv \sum_{\sigma\sigma'} d_{\sigma}^{\dagger} (\boldsymbol{\sigma}_{\sigma\sigma'} / 2) d_{\sigma'}$, where $\boldsymbol{\sigma} \equiv (\sigma_x, \sigma_y, \sigma_z)$ represents the vector of Pauli matrices. J describes the spin-exchange coupling between spin \mathbf{s} of OL electrons and the local spin \mathbf{S} of the molecule, which can be either FM ($J > 0$) or AFM ($J < 0$). By introducing the z component S_t^z of the total spin operator $\mathbf{S}_t \equiv \mathbf{s} + \mathbf{S}$, many-body eigenstates of the SMM can be written as $|n, S_t; S_t^z\rangle$, where n denotes the charge state of the SMM and S_t is the quantum number of the total spin \mathbf{S}_t .

The second term of Eq.(1) describes noninteracting electrons in the electrodes, $H_{leads} = \sum_{\alpha=L,R} \sum_{\mathbf{k}\sigma} \varepsilon_{\alpha\mathbf{k}\sigma} c_{\alpha\mathbf{k}\sigma}^{\dagger} c_{\alpha\mathbf{k}\sigma}$, where $\varepsilon_{\alpha\mathbf{k}\sigma}$ is the energy of an electron with wave vector \mathbf{k} and spin σ in lead α , and $c_{\alpha\mathbf{k}\sigma}^{\dagger}$ ($c_{\alpha\mathbf{k}\sigma}$) is the corresponding electronic creation (annihilation) operator. Assuming $\rho_{\alpha\sigma}$ is the density of states of electrons with spin σ in the lead α , we can define the spin polarization of the ferromagnetic lead as $p_{\alpha} = (\rho_{\alpha\uparrow} - \rho_{\alpha\downarrow}) / (\rho_{\alpha\uparrow} + \rho_{\alpha\downarrow})$. In our calculation, polarizations of the left FM and right NM leads are chosen as $p_L = 0.4$ and $p_R = 0$, respectively, where $p_L = 0.4$ is the typical spin polarization in ferromagnetic systems.

The coupling between the leads and the SMM is described by the tunneling Hamiltonian $H_T = \sum_{\alpha\mathbf{k}\sigma} (t_{\alpha} c_{\alpha\mathbf{k}\sigma}^{\dagger} d_{\sigma} + t_{\alpha}^{*} d_{\sigma}^{\dagger} c_{\alpha\mathbf{k}\sigma})$, where t_{α} is the tunnel matrix element between the lead α and the SMM, and the spin-dependent tunnel-coupling strength is denoted by $\Gamma_{\alpha\sigma} = 2\pi\rho_{\alpha\sigma} |t_{\alpha}|^2$. Furthermore, we can rewrite the tunnel-coupling strength as $\Gamma_{\alpha\sigma} = \Gamma_{\alpha}(1 \pm p_{\alpha})/2$ with the sign $+$ ($-$) corresponding to $\sigma = \uparrow$ (\downarrow), and assume $\Gamma_{\alpha} = \Gamma_{\alpha\uparrow} + \Gamma_{\alpha\downarrow}$ and $\Gamma = (\Gamma_L + \Gamma_R)/2$. For simplicity, the bias voltage V is applied symmetrically on the SMM tunnel junction with $\mu_L = eV/2$ and $\mu_R = -eV/2$.

We analyze spin-polarized transport through the SMM junction in both sequential and cotunneling regimes at the weak-coupling limit, ie. $\Gamma \ll k_B T$. The tunneling processes of electron are assumed to be stochastic and

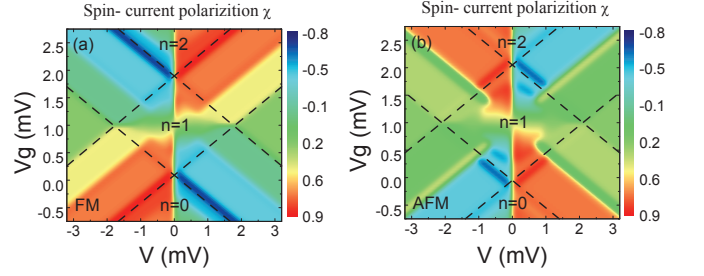


FIG. 2: (Color online) Spin-current polarization for the FM (a) and AFM (b) exchange couplings as a function of the bias and gate voltages. The parameters are: $S = 2$, $\varepsilon = 0.5$ meV, $|J| = 0.4$ meV, $U = 1$ meV, $K = 0.05$ meV, $k_B T = 0.04$ meV, $P_L = 0.4$, $P_R = 0$, and $\Gamma = \Gamma_L = \Gamma_R = 0.001$ meV.

Markovian, and the time evolution of the SMM can be described by the master equation,^{21,33-35}

$$\frac{dP_i}{dt} = \sum_{\alpha\alpha'\sigma\sigma' i' \neq i} [-(W_{\alpha\sigma}^{i,i'} + W_{\alpha\sigma}^{i,i'})P_i + (W_{\alpha\sigma}^{i',i} + W_{\alpha\sigma'}^{i',i})P_{i'}], \quad (3)$$

with P_i denoting the probability in the molecular many-body eigenstate $|i\rangle$. The transition rates W in the Eq. (3) can be calculated perturbatively by the generalized Fermi's golden rule based on the T -matrix.³⁶ Moreover, the rate $W_{\alpha\sigma}^{i,i'}$ denotes the sequential tunneling transition from the state $|i\rangle$ to $|i'\rangle$ due to a spin- σ electron tunneling of lead α , and $W_{\alpha\sigma,\alpha'\sigma'}^{i,i'}$ stands for the cotunneling transition with a spin- σ electron of lead α being transformed to spin- σ' electron of lead α' , respectively. With the stationary conditions $\frac{dP_i}{dt} = 0$ and $\sum_i P_i = 1$, we can get the steady state transport properties. Finally, the current of spin- σ electrons through lead α is defined as^{33,35}

$$I_{\alpha\sigma} = e(-1)^{\delta_{R\alpha}} \sum_{\alpha' \neq \alpha \sigma' i i'} [(n_{i'} - n_i) W_{\alpha\sigma}^{i,i'} P_i + (W_{\alpha\sigma,\alpha'\sigma'}^{i,i'} - W_{\alpha'\sigma',\alpha\sigma}^{i,i'}) P_i], \quad (4)$$

and thus we have the total charge current $I_{\alpha} = I_{\alpha\uparrow} + I_{\alpha\downarrow}$ as well as the spin-current $I_{\alpha s} = I_{\alpha\uparrow} - I_{\alpha\downarrow}$. The polarization of spin-current is defined as

$$\chi = (I_{\alpha\uparrow} - I_{\alpha\downarrow}) / (I_{\alpha\uparrow} + I_{\alpha\downarrow})$$

In addition, magnetization of the SMM is $\langle S_t^z \rangle = \sum_i S_{ii}^z P_i$. With this well-defined theory, we can calculate the spin transport properties of the SMM junction and the results are presented below.

III. RESULTS AND DISCUSSION

In Fig. 2, we show the dependence of the spin-current polarization on the gate and bias voltages for the FM

and AFM spin-exchange couplings. We first find that the polarization χ is asymmetric under reversal of the bias voltage V , since tunnel-coupling strengths between the molecule and the FM electrode is spin-dependent ($\Gamma_{L\uparrow} > \Gamma_{L\downarrow}$). At lower bias voltages, the cotunneling processes dominates electron transports in the regions marked by the electron occupation numbers $n = 0$ (1 or 2),^{20,21} and the sequential tunneling processes start to take part in transports at larger bias voltages. Although the polarization of FM lead is 0.4, the spin-current polarization χ can be beyond 0.4, or even more than 0.8 in the sequential and cotunneling regions [Figs. 2(a) and (b)]. Moreover, because the energy of the molecular state $|1, 5/2; S_t^z\rangle$ is larger than that of the molecular state $|1, 3/2; S_t^z\rangle$ for the AFM case,³³ the voltage-dependence of spin-polarization χ is very different for the two types of couplings, or even opposite in some regions.

The charge current I_c , spin current I_s , differential conductance G , magnetization $\langle S_t^z \rangle$, and spin polarization χ are shown in Fig. 3 for the FM spin-exchange coupling. The spin-flip induced by the spin-exchange coupling plays a key role^{20,21,25,33} in the quantum transport through the SMM. The magnetization $\langle S_t^z \rangle$ is a positive value in the negative bias voltages [Fig. 3(c)], since the states with positive S_t^z dominate the steady transport processes. It becomes negative in the positive bias voltages. The charge current I_c (black solid line) and spin current I_s (red dash line) versus the bias voltage V are shown in Fig. 3(a) at the gate voltage $V_g = -0.4$ mV, where the degenerate ground states of the SMM are $|0, 2; \pm 2\rangle$. The spin current I_s is negative at most of bias voltage region except the high positive-bias, where all the transport channels are open. The variation of differential conductance G with respect to the bias voltage V is plotted in Fig. 3(b), which displays three sequential resonant peaks in the positive bias. The peak-1 corresponds to the spin-down sequential transition $|0, 2; -2\rangle \Leftrightarrow |1, 5/2; -5/2\rangle$, and the peak-2 (peak-3) corresponds to the spin-up transition $|0, 2; -2\rangle \Leftrightarrow |1, 3/2; -3/2\rangle$ ($|1, 5/2; -5/2\rangle \Leftrightarrow |2, 2; -2\rangle$). In the negative bias, the peak-1' corresponds to the spin-up transition $|0, 2; 2\rangle \Leftrightarrow |1, 5/2; 5/2\rangle$, and the peak-2' (peak-3') corresponds to the spin-down transition $|0, 2; 2\rangle \Leftrightarrow |1, 3/2; 3/2\rangle$ ($|1, 5/2; 5/2\rangle \Leftrightarrow |2, 2; 2\rangle$). The height of peak-1 is lower than that of the peak-1', since spin-up (spin-down) electrons are majority (minority) in the L -electrode.

The spin-current polarization χ as a function of the bias voltage V is shown in Fig. 3(d) for different gate voltages. At low bias voltages around $V = 0$ mV, the electron transport is dominated by elastic cotunneling processes and thus the polarization χ approaches the spin polarization of FM lead, namely $\chi \sim 0.4$. With the slight increase of bias voltage V , the inelastic cotunneling processes start to take part in electron transports. For the gate voltage $V_g = -0.4$ mV (black solid line), at positive bias the transport current is brought mainly by the spin-down electrons tunneling through the SMM via the virtual transition $|0, 2; -2\rangle \Leftrightarrow |1, 5/2; -5/2\rangle$,²⁰ and the

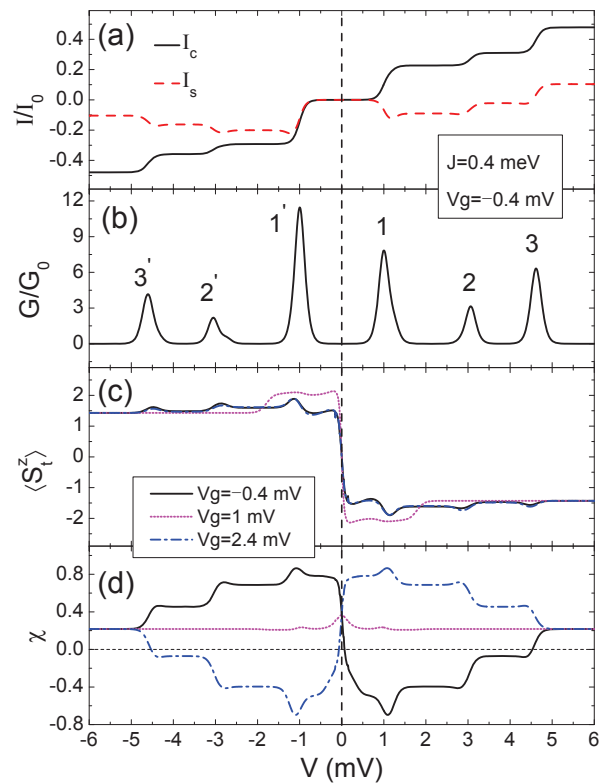


FIG. 3: (Color online) In the case of FM exchange coupling ($J = 0.4$ meV): (a) charge current I_c and spin current I_s , (b) differential conductance G , (c) magnetization $\langle S_t^z \rangle$, and (d) spin-current polarization χ as a function of the bias voltage V for different gate voltages V_g . The current and differential conductance are scaled in units of $I_0 = 2e\Gamma/h$ and $G_0 = 10^{-3}e^2/h$, respectively.

polarization χ is from positive values to negative values. At negative bias, the transport is dominated by the spin-up (spin-majority) electrons tunneling via the virtual transition $|0, 2; 2\rangle \Leftrightarrow |1, 5/2; 5/2\rangle$, and the polarization χ is enhanced, larger than 0.8. When the bias voltage increases further to the threshold value, sequential tunneling begins to dominate the electron transports. The polarization reaches the lowest value $\chi \sim -0.7$ at the peak-1 of differential conductance as displayed in Fig. 3 (b), where the transport is dominated by spin-down electrons. It reduces to -0.4 (-0.1) approximately between the peak-1 and peak-2 (peak-2 and peak-3), where more spin-up electrons take part in the transport. On the other hand, the polarization χ at the conductance peak-1' obtains the highest value about 0.9, where the spin-up electrons dominate the transport. It reduces to about 0.7 (0.4) between the peak-1' and peak-2' (peak-2' and peak-3'). When the absolute value of bias-voltage V is high enough, all transition channels enter the transport window and the polarization χ remains in a constant magnitude close to 0.2. This situation is the same as in the QDs.⁷ At the gate voltage $V_g = 1$ mV the ground states

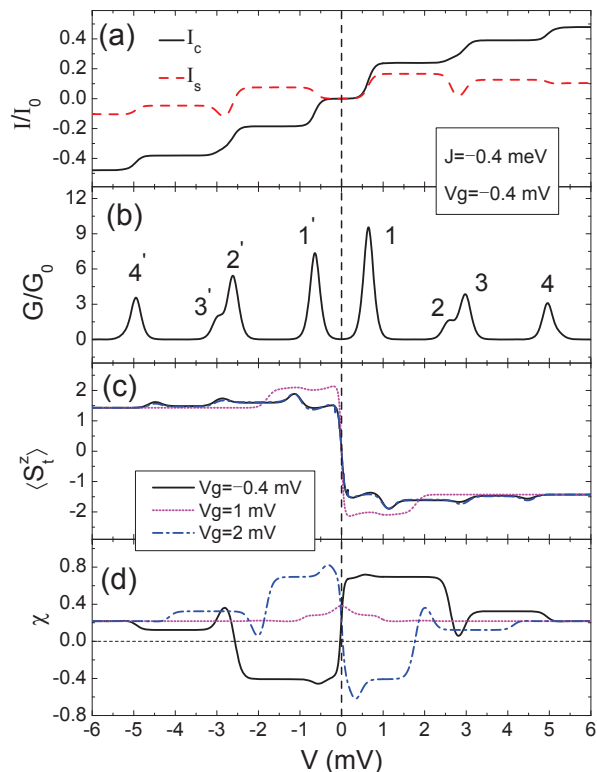


FIG. 4: (Color online) In the case of AFM exchange coupling ($J = -0.4$ meV): (a) charge current I_c and spin current I_s , (b) differential conductance G , (c) magnetization $\langle S_t^z \rangle$, and (d) spin-current polarization χ as a function of the bias voltage V for different gate voltages V_g .

of SMM become $|1, 5/2; \pm 5/2\rangle$, where the spin polarization curve χ (pink dash line) varies approximately from 0.4 to 0.2 with increasing bias V . Since the gate voltages $V_g = 2.4$ mV and $V_g = -0.4$ mV are symmetric with respect to $V_g = 1$ mV, which is the electron-hole symmetry point,^{20,25} the corresponding polarization curves (blue dot-dash and black solid lines) exhibit a symmetric behavior seen from Fig. 3(d). For $V_g = 2.4$ mV, the highest polarization χ located at peak-1 is mainly contributed by the spin-up transitions $|2, 2; -2\rangle \Leftrightarrow |1, 5/2; -5/2\rangle$.

Figure 4 presents the spin-polarized transport through the SMM tunnel junction with the AFM exchange interaction between the conduction electrons and the molecular giant-spin. Different from the FM case, the polarization χ at the gate voltage $V_g = -0.4$ mV increases from 0.4 to about 0.7 in the positive bias. This behavior is attributed to the spin-up virtual transition $|0, 2; -2\rangle \Leftrightarrow |1, 3/2; -3/2\rangle$. While χ decreases to the

negative value about -0.4 in the negative bias due to the spin-down virtual transition $|0, 2; 2\rangle \Leftrightarrow |1, 3/2; 3/2\rangle$. When the bias voltage increases to a certain higher value, the sequential tunneling dominates the electronic transport, and the differential conductance G possesses four peaks for both positive and negative bias voltages, as shown in Fig. 4(b). The peak-1 mainly from the transitions $|0, 2; -2\rangle \Leftrightarrow |1, 3/2; -3/2\rangle$ is higher than the peak-1', which is contributed by the transitions $|0, 2; 2\rangle \Leftrightarrow |1, 3/2; 3/2\rangle$. The corresponding polarization χ at peak-1 (peak-1') reaches the highest (lowest) value about 0.7 (-0.4). The conductance peak-2 and peak-3 are related to the transitions $|0, 2; -2\rangle \Leftrightarrow |1, 5/2; -5/2\rangle$ and $|1, 5/2; -5/2\rangle \Leftrightarrow |2, 2; -2\rangle$ respectively, and a small dip appears for the polarization curve (black solid line) between the two peaks. In contrast, the polarization curve is convex between the peak-2' and peak-3'. Additional peak-4 and peak-4' emerge with further increase of the bias voltage V . These two peaks are mainly contributed from the transitions $|1, 3/2; -3/2\rangle \Leftrightarrow |2, 2; -2\rangle$ and $|1, 3/2; 3/2\rangle \Leftrightarrow |2, 2; 2\rangle$ respectively. More interestingly, without the reversal of bias, the polarization χ for $V_g = 2$ mV (blue dot-dash line) can be reversed from about -0.6 to 0.4 in positive bias range.

IV. CONCLUSION

In conclusion, we have shown that the FM-SMM-NM junction can work as an efficient spin-current injector. By the quantum master equation approach, the spin-polarized transport properties are systematically investigated in both the sequential and cotunneling regimes. Our results demonstrate that the transport exhibits a very asymmetric behavior with respect to the zero bias. The spin-flip process, which originates from the spin-exchange interaction of the SMM and the transport electron, leads to the amplification of spin polarization injecting from the FM electrode, and a very high polarization of the spin-current is obtained. Furthermore, both the magnitude and sign of the spin polarization are tunable by the gate or bias voltages, suggesting an electrically-controllable spin device in molecular spintronics.

Acknowledgments

This work was supported by National Natural Science Foundation of China under grant Nos. 11504260, 11447163, 11574186, 11275118, 11504240, and STIP under grant Nos. 2014147, 2016170.

* Electronic address: xufuming@szu.edu.cn

† Electronic address: q2wang332@163.com

¹ I. Žutić, J. Fabian, and S. D. Sarma, Rev. Mod. Phys. 76,

323 (2004).

² W. Han, K. Pi, K. M. McCreary, Y. Li, J. J. I. Wong, A. G. Swartz, and R. K. Kawakami, Phys. Rev. Lett. 105,

- 167202 (2010).
- ³ C. Zhang, Y. Wang, B. Wu, and Y. Wu, *Appl. Phys. Lett.* 101, 022406 (2012).
 - ⁴ L. K. Castelano and L. J. Sham, *Appl. Phys. Lett.* 96, 212107 (2010).
 - ⁵ C. A. Merchant and N. Markovic, *Phys. Rev. Lett.* 100, 156601 (2008).
 - ⁶ K. Hamaya, M. Kitabatake, K. Shibata, M. Jung, S. Ishida, T. Taniyama, K. Hirakawa, Y. Arakawa, and T. Machida, *Phys. Rev. Lett.* 102, 236806 (2009).
 - ⁷ F. M. Souza, J. C. Egues, and A. P. Jauho, *Phys. Rev. B* 75, 165303 (2007).
 - ⁸ S. Csonka, I. Weymann, and G. Zarand, *Nanoscale* 4, 3635 (2012).
 - ⁹ R. Meservey and P. M. Tedrow, *Phys. Rep.* 238, 173 (1994).
 - ¹⁰ L. Bogani and W. Wernsdorfer, *Nature Mater.* 7, 179 (2008).
 - ¹¹ H. B. Heersche, Z. de Groot, J. A. Folk, H. S. J. van der Zant, C. Romeike, M. R. Wegewijs, L. Zobbi, D. Barreca, E. Tondello, and A. Cornia, *Phys. Rev. Lett.* 96, 206801 (2006).
 - ¹² C. Romeike, M. R. Wegewijs, and H. Schoeller, *Phys. Rev. Lett.* 96, 196805 (2006).
 - ¹³ C. Timm and F. Elste, *Phys. Rev. B* 73, 235304 (2006).
 - ¹⁴ M. Misiorny and J. Barnaś, *Phys. Rev. B* 76, 054448 (2007).
 - ¹⁵ F. Delgado and J. Fernández-Rossier, *Phys. Rev. B* 82, 134414 (2010).
 - ¹⁶ H.-Z. Lu, B. Zhou, and S.-Q. Shen, *Phys. Rev. B* 79, 174419 (2009).
 - ¹⁷ Z. Zhang, L. Jiang, R. Wang, B. Wang, and D. Y. Xing, *Appl. Phys. Lett.* 99, 133110 (2011).
 - ¹⁸ M. Misiorny and J. Barnaś, *Phys. Rev. Lett.* 111, 046603 (2013).
 - ¹⁹ S. Loth, K. von Bergmann, M. Ternes, A. F. Otte, C. P. Lutz, and A. J. Heinrich, *Nat. Phys.* 6, 340 (2010).
 - ²⁰ M. Misiorny and J. Barnaś, *Phys. Rev. B* 79, 224420 (2009);
 - ²¹ H. Xie, Q. Wang, H. B. Xue, H. Jiao and J.-Q. Liang, *J. Appl. Phys.* 113, 213708 (2013).
 - ²² M. Misiorny, I. Weymann, and J. Barnaś, *Phys. Rev. Lett.* 106, 126602 (2011)
 - ²³ M. Misiorny, I. Weymann, and J. Barnaś, *Phys. Rev. B* 84, 035445 (2011).
 - ²⁴ F. D. Natterer, K. Yang, W. Paul, P. Willke, T. Choi, T. Greber, A. J. Heinrich, and C. P. Lutz, *Nature* 543, 226 (2017).
 - ²⁵ M. Misiorny and J. Barnaś, *Europhys. Lett.* 89, 18003 (2010).
 - ²⁶ H.-B. Xue, J.-Q. Liang, and W.-M. Liu, *Sci. Rep.* 5, 8730 (2015).
 - ²⁷ C. Timm and M. Di Ventura, *Phys. Rev. B* 86, 104427 (2012).
 - ²⁸ L. Zhu, K. L. Yao, and Z. L. Liu, *Appl. Phys. Lett.* 96, 082115 (2010).
 - ²⁹ H. Hao, X. H. Zheng, Z. X. Dai, and Z. Zeng, *Appl. Phys. Lett.* 96, 192112 (2010).
 - ³⁰ R.-Q. Wang, L. Sheng, R. Shen, B. Wang, and D.Y. Xing, *Phys. Rev. Lett.* 105, 057202 (2010);
 - ³¹ Z. Zhang, L. Jiang, R. Wang, B. Wang, and D. Y. Xing, *Appl. Phys. Lett.* 97, 242101 (2010).
 - ³² H. Xie, Q. Wang, H. Jiao, and J.-Q. Liang, *J. Appl. Phys.* 112, 043701 (2012).
 - ³³ H. Xie, Q. Wang, B. Chang, H. Jiao, and J.-Q. Liang, *J. Appl. Phys.* 111, 063707 (2012).
 - ³⁴ C. Timm, *Phys. Rev. B* 77, 195416 (2008).
 - ³⁵ J. Koch, F. von Oppen, and A. V. Andreev, *Phys. Rev. B* 74, 205438 (2006).
 - ³⁶ H. Bruus and K. Flensberg, *Many-body Quantum Theory in Condensed Matter Physics* (Oxford University Press, Oxford, 2004).